Upper critical field and thermally activated flux flow in single-crystalline $Tl_{0.58}Rb_{0.42}Fe_{1.72}Se_2$

L. Jiao,[1] Y. Kohama,[2] J. L. Zhang,[1] H. D. Wang,[1,3] B. Maiorov,[2] F. F. Balakirev,[2] Y. Chen,[1] L. N. Wang,[1] T. Shang,[1] M. H. Fang,[1] and H. Q. Yuan[1,*]

[1]*Department of Physics, Zhejiang University, Hangzhou, Zhejiang 310027, China*
[2]*Los Alamos National Laboratory, Los Alamos, New Mexico 87545, USA*
[3]*Department of Physics, Hangzhou Normal University, Hangzhou, Zhejiang 310036, China*

(Received 11 June 2011; revised manuscript received 8 November 2011; published 15 February 2012)

The upper critical field $\mu_0 H_{c2}(T_c)$ of $Tl_{0.58}Rb_{0.42}Fe_{1.72}Se_2$ single crystals has been determined by means of measuring the electrical resistivity in both a pulsed magnetic field (∼58 T) and a dc magnetic field (∼14 T). It is found that $\mu_0 H_{c2}$ linearly increases with decreasing temperature for $\mathbf{H} \parallel c$, reaching $\mu_0 H_{c2}^{\mathbf{H}\parallel c}(0\ \mathrm{K}) \simeq 60$ T. On the other hand, a larger $\mu_0 H_{c2}(0\ \mathrm{K})$ with a strong convex curvature is observed for $\mathbf{H} \perp c$ [$\mu_0 H_{c2}^{\mathbf{H}\perp c}(18\ \mathrm{K}) \simeq 60$ T]. This compound shows a moderate anisotropy of the upper critical field around T_c, which decreases with decreasing temperature. Analysis of the upper critical field based on the Werthamer-Helfand-Hohenberg (WHH) method indicates that $\mu_0 H_{c2}(0\ \mathrm{K})$ is orbitally limited for $\mathbf{H} \parallel c$, but the effect of spin paramagnetism may play an important role in the pair breaking for $\mathbf{H} \perp c$. All these experimental observations remarkably resemble those of the iron pnictide superconductors, suggesting a universal scenario for the iron-based superconductors. Moreover, the superconducting transition is broadened significantly upon applying a magnetic field, indicating strong thermal fluctuation effects in the superconducting state of $Tl_{0.58}Rb_{0.42}Fe_{1.72}Se_2$. The derived thermal activation energy for vortex motion is compatible with those of the 1111-type iron pnictides.

DOI: 10.1103/PhysRevB.85.064513 PACS number(s): 74.70.Xa, 71.35.Ji, 74.25.Op

I. INTRODUCTION

The newly discovered Fe-based superconductors (FeSCs) share many similarities with the high-T_c cuprates,[1] e.g., both showing a relatively high superconducting transition temperature T_c and possessing a layered crystal structure. It is, therefore, natural to compare these two classes of superconductors, which might help unravel the puzzles of high-T_c superconductivity. However, significantly distinct properties have been demonstrated in the FeSCs,[1] including that (i) most of the parent compounds of FeSCs are typically bad metal instead of a Mott insulator as found in the cuprates; (ii) the FeSCs are a multiband system, which seems to favor a $s^{\pm}$-pairing state rather than a d-wave state; (iii) both the FeSCs and the cuprates possess a very large upper critical field, but the FeSCs show nearly isotropic H_{c2} at low temperatures despite their layered crystal structures. Clarification of the electronic coupling strength in FeSCs is the basis for establishing a pertinent theory of superconductivity. Various approaches, either based on the Fermi-surface nesting[2] or started from the proximity to a Mott insulator[3] initially were proposed to reveal the physics of iron pnictides, but no consensus has been reached. Recently, dual characters of localized and itinerant $3d$ electrons theoretically were proposed[4] and experimentally were shown in some iron pnictides.[5,6] To reveal the nature of magnetism and superconductivity in FeSCs and to compare it with the high-T_c cuprates, it remains highly desired to search for FeSCs near a Mott insulator.

Very recently, a new class of FeSCs, $A\mathrm{Fe}_x\mathrm{Se}_2$ [A = K,[7] Cs,[8] Rb,[9] ($Tl_{1-y}K_y$) (Ref. 10) and ($Tl_{1-y}Rb_y$) (Ref. 11)], was discovered with T_c up to ∼33 K. Remarkably different from the iron pnictides, superconductivity in iron selenides seems to develop from an antiferromagnetic Mott insulator with a rather high Néel temperature.[10–15] In these compounds, one may tune the interplay of superconductivity and magnetism by changing the Fe-vacancy order.[10,14,15] Furthermore, the reported angle-resolved photoemission spectroscopy (ARPES) experiments on iron selenides showed that an isotropic superconducting gap emerged around the electron pocket at the M point, but the hole band centered at the Γ point sinks below the Fermi level.[16–18] This is in sharp contrast to that of the iron pnictide superconductors in which both hole and electron pockets, connected with a nesting wave vector, were experimentally observed.[19] It is, therefore, of great interest to find out whether the iron selenide superconductors represent a new type of FeSCs (e.g., similar to the high-T_c cuprates) or remain similar to other iron pnictides. In any case, the iron selenide superconductors may provide an alternative example for studying the pairing mechanisms of high-T_c superconductivity, in particular, for the FeSCs. To elucidate the above issues, it is highly important to compare the main superconducting parameters of the iron selenides with those of the iron pnictides and with those among the iron selenide series.

In this paper, we report measurements of the electrical resistivity in both a pulsed magnetic field and a dc magnetic field for the single-crystalline $Tl_{0.58}Rb_{0.42}Fe_{1.72}Se_2$. It is found that $Tl_{0.58}Rb_{0.42}Fe_{1.72}Se_2$ shows a very large upper critical field [$\mu_0 H_{c2}^{\mathbf{H}\parallel c}(0\ \mathrm{K}) \simeq 60$ T, $\mu_0 H_{c2}^{\mathbf{H}\perp c}(18\ \mathrm{K}) \simeq 60$ T] with a moderate anisotropic parameter γ ($\gamma = H_{c2}^{\mathbf{H}\perp c}/H_{c2}^{\mathbf{H}\parallel c}$), remarkably resembling those of iron pnictide superconductors.[20–25] On the other hand, the superconducting transition of $Tl_{0.58}Rb_{0.42}Fe_{1.72}Se_2$ is broadened substantially in a magnetic field, indicating significant contributions of a thermally activated flux flow in the vortex state.

II. EXPERIMENTAL METHODS

Single crystals of $Tl_{0.58}Rb_{0.42}Fe_{1.72}Se_2$ were synthesized by using the Bridgeman method.[11] The x-ray diffraction identified the derived samples as a single phase with a tetragonal $ThCr_2Si_2$ crystal structure. The actual composition of the crystals was determined by energy dispersive x-ray spectrometer. Magnetic-field dependence of the electrical resistivity $\rho(H)$ was measured up to 58 T using a typical four-probe method in a capacitor-bank-driven pulsed magnet. The experimental data were recorded on a digitizer using a custom-designed high-resolution low-noise synchronous lock-in technique. In order to minimize the eddy-current heating caused by the pulsed magnetic field, very small crystals were cleaved off along the *ab* plane from the as-grown samples. The electrical resistivity in a dc magnetic field (0–14 T) was measured in an Oxford Instruments HELIOX VL system using a Lakeshore ac resistance bridge, and the angular dependence of the electrical resistivity was performed in a quantum design (QD) physical properties measurement system (9 T). Angular linear transport measurements (ρ) were carried out using the maximum Lorentz force configuration ($\mathbf{J} \perp \mathbf{H}$) with $\mathbf{H}$ applied at an angle θ from the c axis of the crystal (see the inset of Fig. 5).

III. THE UPPER CRITICAL FIELD AND ITS ANISOTROPY

In Fig. 1, we show the temperature dependence of the electrical resistivity in a zero field for $Tl_{0.58}Rb_{0.42}Fe_{1.72}Se_2$ (#1). One can see that the resistivity $\rho(T)$ shows a hump around 154 K, changing from semiconducting to metallic behavior upon cooling down from room temperature. Such a hump in $\rho(T)$ has been observed widely in the iron selenides,[7–12,26] and its position can be tuned either by doping[12] or by pressure.[26] The origin of the hump and its relation to superconductivity remain unclear. A very sharp superconducting transition shows up at $T_c \simeq 33.5$ K, indicating the high quality of the sample. Note that we have totally measured four samples cut from the same batch in this context and their T_c only varies slightly from 32.9 to 33.5 K, indicating a good reproducibility of the superconducting properties in these samples.

Figures 2 and 3 show the temperature and the magnetic-field dependence of the electrical resistivity for $Tl_{0.58}Rb_{0.42}Fe_{1.72}Se_2$, respectively. In order to study the anisotropic behavior, the electrical resistivity was measured with the field (a) perpendicular and (b) parallel to the c axis.

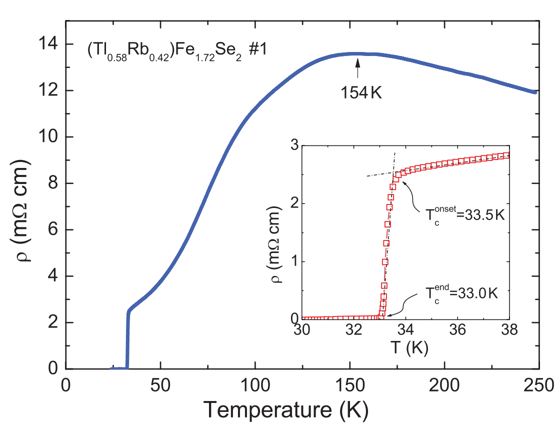

FIG. 1. (Color online) Temperature dependence of the electrical resistivity $\rho(T)$ at $\mu_0 H = 0$ for $Tl_{0.58}Rb_{0.42}Fe_{1.72}Se_2$ (#1). The inset enlarges the section of the superconducting transition where $T_c^{\text{onset}} \simeq 33.5$ and $T_c^{\text{end}} \simeq 33$ K are determined from the onset and the end point of the superconducting transition, respectively.

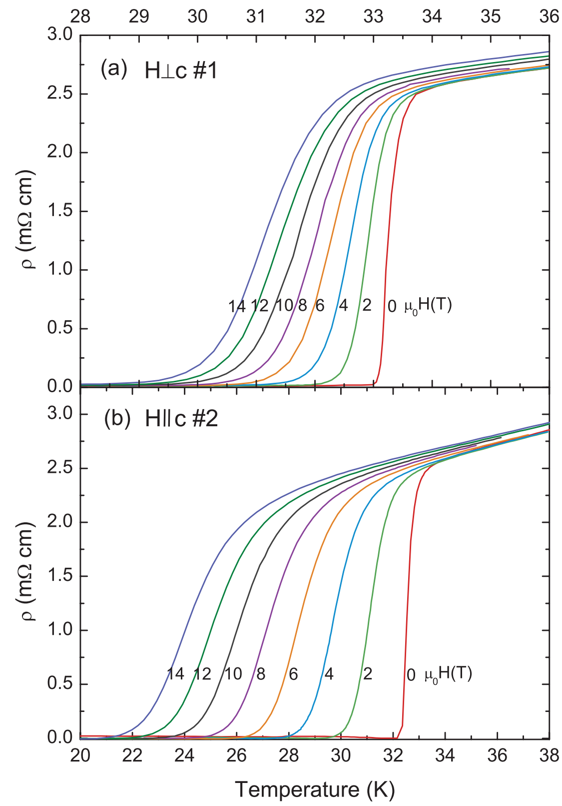

FIG. 2. (Color online) Temperature dependence of the electrical resistivity $\rho(T)$ for $Tl_{0.58}Rb_{0.42}Fe_{1.72}Se_2$ (#1 and #2) measured in dc fields up to 14 T: (a) $\mathbf{H} \perp c$; (b) $\mathbf{H} \parallel c$.

The magnetic field is applied up to 14 T for the dc fields (Fig. 2) and up to 58 T for the pulsed magnetic fields (Fig. 3). Obviously, the superconducting transition eventually shifts to lower temperatures upon applying a magnetic field. However, superconductivity is remarkably robust against the magnetic field in $Tl_{0.58}Rb_{0.42}Fe_{1.72}Se_2$, and it is not yet completely suppressed at our maximum field of 58 T. Furthermore, one can see that the superconducting transition is broadened significantly upon applying a magnetic field, showing a tail structure at low temperatures. For example, the width of the superconducting transition, defined from the onset temperature to the end point of the superconducting transition (see the inset of Fig. 1), is as small as 0.5 K in the zero field but increases to 2 and 3.6 K for $\mathbf{H} \perp c$ and $\mathbf{H} \parallel c$ at 14 T, respectively. Similar features also were observed in some 1111-type iron pnictides.[27–29] We will argue later that such behavior might be attributed to the thermally activated flux flow in the vortex state. In the normal state, $Tl_{0.58}Rb_{0.42}Fe_{1.72}Se_2$ shows significant positive magnetoresistance for both $\mathbf{H} \parallel c$ and $\mathbf{H} \perp c$. It is noted that, in iron pnictides, the magnetoresistance becomes very high while entering the magnetic state but is negligible in the nonmagnetic state.[5] One possibility for the occurrence of such a high magnetoresistance in $Tl_{0.58}Rb_{0.42}Fe_{1.72}Se_2$ might be related to its magnetic ordering at high temperatures.[14,15]

The upper critical field $\mu_0 H_{c2}(T_c)$ of $Tl_{0.58}Rb_{0.42}Fe_{1.72}Se_2$ is shown in Fig. 4 in which various symbols represent either different field orientations for the same sample (#3) or different samples as marked in the figure. In Fig. 4(a), we determine the critical temperatures T_{c2} (in the case of the dc field) or the

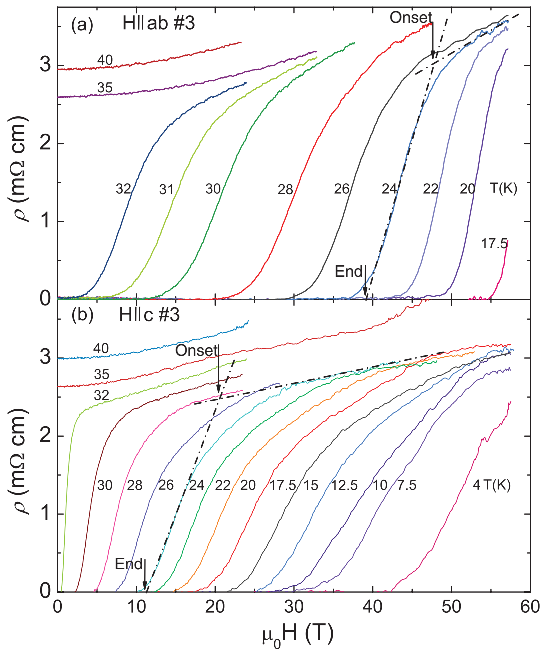

FIG. 3. (Color online) Magnetic-field dependence of the electrical resistivity $\rho(\mu_0 H)$ at various temperatures for $Tl_{0.58}Rb_{0.42}Fe_{1.72}Se_2$ (#3): (a) $\mathbf{H} \perp c$; (b) $\mathbf{H} \parallel c$.

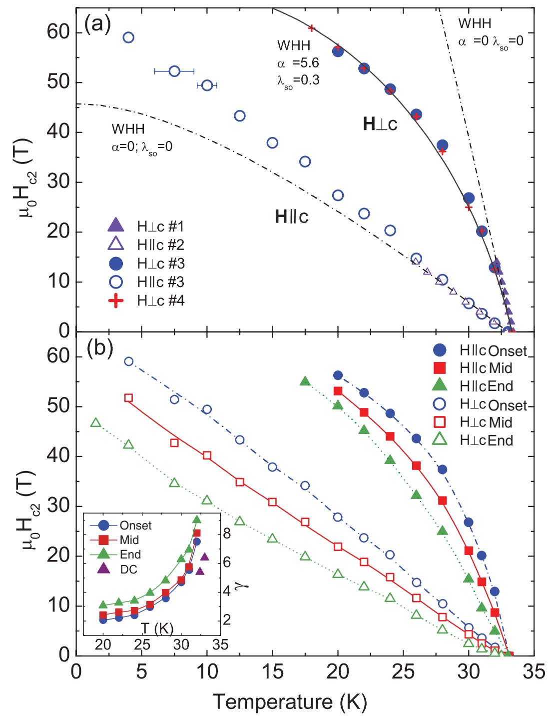

FIG. 4. (Color online) The upper critical field $\mu_0 H_{c2}(T_c)$ for $Tl_{0.58}Rb_{0.42}Fe_{1.72}Se_2$. (a) The values of $\mu_0 H_{c2}(T_c)$ are determined from the superconducting onsets as described in Figs. 1 and 3. Symbols of the open circles (○), filled circles (•), and crosses (+) represent the data obtained in a pulsed magnetic field, and the triangles (△ and ▲) denote those measured in a dc magnetic field. Note that samples #3 and #4 were measured in a pulsed field, but only sample #3 was measured successfully for both $\mathbf{H} \perp c$ and $\mathbf{H} \parallel c$. (b) The values of $\mu_0 H_{c2}(T_c)$ are determined from the onset (○), the min point (□), and the end point (△) of the resistive superconducting transitions (sample # 3), respectively. The inset shows the corresponding temperature dependence of the anisotropic parameter $\gamma(T)$.

critical fields $\mu_0 H_{c2}$ (in the case of the pulsed field) from the superconducting onsets as described in the inset of Fig. 1 and in Fig. 3, i.e., the intersection point of the resistive curves in the normal state and the superconducting transition. Such a determination of $\mu_0 H_{c2}$ (or T_{c2}) is appropriate for the in-field measurements and is particularly useful in the presence of the magnetoresistance $\rho(\mu_0 H)$. In this case, one can extrapolate $\rho(\mu_0 H)$ to lower temperatures to determine $\mu_0 H_{c2}$ at the lowest temperatures since $\rho(\mu_0 H)$ in the normal state hardly depends on temperature. It is noted that similar field-induced broadening of the resistive superconducting transition also was observed in the high-T_c cuprates in which the onset temperature, as we described here, was shown to be close to that determined by other bulk measurements, e.g., the magnetization.[30] From Fig. 4(a), one can see that the derived $\mu_0 H_{c2}(T_c)$ quantitatively demonstrates the same behavior for all the investigated samples, independent of the detailed experimental methods. The upper critical field $\mu_0 H_{c2}^{\mathbf{H}\parallel c}(T_c)$ linearly increases with decreasing temperature, reaching a value of $\mu_0 H_{c2}^{\mathbf{H}\parallel c}(0\text{ K}) \simeq 60$ T. On the other hand, $\mu_0 H_{c2}^{\mathbf{H}\perp c}(T_c)$ shows a convex curvature with a much larger value at low temperatures. Such behavior of $\mu_0 H_{c2}(T_c)$ is not changed by the field-induced broadening of the superconducting transition. Taking sample #3 as an example, in Fig. 4(b), we plot the upper critical fields $\mu_0 H_{c2}(T_c)$ determined at the onset, mid, and end point of the resistive transitions (see Fig. 3), which follow remarkably similar temperature dependence. We note that our results are consistent with those of $K_{0.8}Fe_{1.76}Se_2$ (Ref. 31) and $K_{0.76}Fe_{1.61}Se_{0.96}S_{1.04}$;[32] the former was measured using a tunnel-diode resonator (TDR) technique in a pulsed magnetic field, and the latter was measured only up to 9 T. It also was shown that the values of $\mu_0 H_{c2}$, determined from the end point of the resistive transitions and the TDR technique, are consistent,[31] further confirming the validity of our methods in the determination of the upper critical fields.

In a superconductor, the Cooper pairs can be destroyed by the following two mechanisms in a magnetic field: (i) the orbital-pair breaking due to the Lorentz force acting via the charge on the momenta of the paired electrons (orbital limit) and (ii) the Zeeman effect aligning the spins of the two electrons with the applied field (Pauli paramagnetic limit). According to the WHH method, the orbital-limiting upper critical field $\mu_0 H_{c2}^{\text{orb}}(0\text{ K})$ for a single-band BCS superconductor is determined by the initial slope of $\mu_0 H_{c2}(T_c)$ at T_c, i.e.,[33]

$$\mu_0 H_{c2}^{\text{orb}}(0\text{ K}) = -0.69 T_c (dH_{c2}/dT)|_{T=T_c}, \qquad (1)$$

whose value may depend on the field orientations. The Pauli paramagnetic limiting field for weakly coupled BCS superconductors is given by[34]

$$\mu_0 H_{c2}^{p}(0\text{ K})\ [\text{T}] = 1.86 T_c\ [\text{K}]. \qquad (2)$$

While the upper critical field usually is restricted by the orbital limit in conventional superconductors, the spin-paramagnetic effect may play an important role in

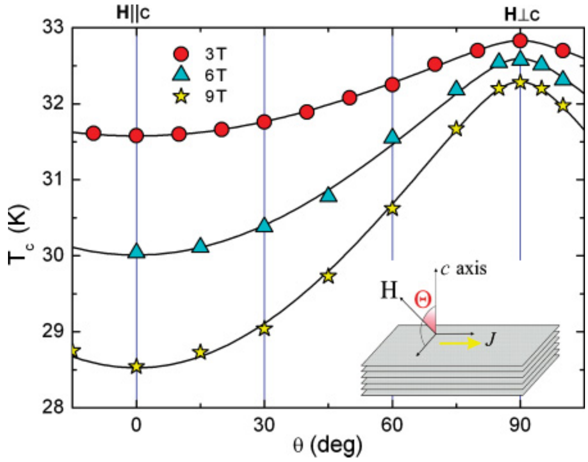

FIG. 5. (Color online) The angular dependence of the superconducting critical temperature $T_c(\theta)$ at magnetic fields of $\mu_0 H = 3$, 6, and 9 T. The solid lines show the fittings to Eq. (4). Here, $T_c(\theta)$ is determined from the superconducting onsets.

pair breaking in some unconventional superconductors. $Tl_{0.58}Rb_{0.42}Fe_{1.72}Se_2$ reveals a relatively large and anisotropic initial slope of $\mu_0 H_{c2}(T_c)$ near T_c, which reaches a value of -12 and -2 T/K (from the superconducting onsets) for $\mathbf{H} \perp c$ and $\mathbf{H} \parallel c$, respectively. Following Eq. (1), one can derive the orbitally limited upper critical field, which gives $\mu_0 H_{c2}^{\mathrm{orb}}(0\ \mathrm{K}) = 273$ T for $\mathbf{H} \perp c$ and 45 T for $\mathbf{H} \parallel c$. As shown in Fig. 4, $\mu_0 H_{c2}^{\mathrm{orb}}(0\ \mathrm{K})$ considerably exceeds the experimental value of $\mu_0 H_{c2}(0\ \mathrm{K})$ for $\mathbf{H} \perp c$ but lightly falls below the corresponding $\mu_0 H_{c2}(0\ \mathrm{K})$ for $\mathbf{H} \parallel c$. On the other hand, Eq. (2) gives a Pauli paramagnetic limiting field of $\mu_0 H_{c2}^{p}(0\ \mathrm{K}) \approx 60$ T in terms of the BCS theory. Thus, it is likely that the upper critical field is limited by the orbital effect for $\mathbf{H} \parallel c$ but by the spin paramagnetic effect for $\mathbf{H} \perp c$. In order to look into this point further, we fitted the experimental data of $\mu_0 H_{c2}(T_c)$ with the WHH model[33] in which the effects of both orbital and spin-pair breakings are considered [see Fig.4(a)]. In this model, α and λ_{so} are the fitting parameters, α is the Maki parameter, which represents the relative strength of spin and orbital pair breakings, and λ_{so} is the spin-orbit scattering constant. As shown in Fig. 4(a), the upper critical field $\mu_0 H_{c2}(T_c)$ for both $\mathbf{H} \parallel c$ and $\mathbf{H} \perp c$ is not described well by the WHH method while ignoring the spin effect (see the dot-dashed lines with $\alpha = 0$ and $\lambda_{\mathrm{so}} = 0$). The enhancement of $\mu_0 H_{c2}^{\mathbf{H}\parallel c}(T_c)$ at low temperatures is likely attributed to its multiband electronic structure as discussed concerning other FeSCs.[25] Indeed, $\mu_0 H_{c2}^{\mathbf{H}\perp c}(T_c)$ can be fitted well by the WHH model after considering the spin effect [see the solid line in Fig.4(a)], which gives $\alpha = 5.6$ and $\lambda_{\mathrm{so}} = 0.3$. Such a large value of α indicates that the spin paramagnetism may play an important role in suppressing superconductivity for $\mathbf{H} \perp c$. A similar analysis applies to the data of $\mu_0 H_{c2}(T_c)$ derived at various resistive drops of the broad superconducting transition, showing generally consistent behavior. In the case of a cylinderlike Fermi surface, the open electron orbits along the c axis make the orbital-limiting upper critical field unlikely. Existence of a Pauli limiting $\mu_0 H_{c2}(0)$ for $H \perp c$ seems to agree with the enhanced anisotropy in $Tl_{0.58}Rb_{0.42}Fe_{1.72}Se_2$ (see below). On the other hand, its multiband electronic structure may complicate the analysis of $\mu_0 H_{c2}(T_c)$. Nevertheless, the upper critical field of $Tl_{0.58}Rb_{0.42}Fe_{1.72}Se_2$ shows a similar behavior to that of other iron pnictide superconductors,[20–25] indicating a uniform scenario of $\mu_0 H_{c2}(0)$ in the FeSCs.

The anisotropic parameter $\gamma(T)$ of $Tl_{0.58}Rb_{0.42}Fe_{1.72}Se_2$ (sample #3), derived at various points of the superconducting transition, is shown in the inset of Fig. 4(b). One can see that all these curves follow exactly same temperature dependence but with a small deviation in their absolute values of $\gamma(T)$. For example, the anisotropic parameter γ, determined from the superconducting onsets, is as high as 8 near T_c but reaches 2 at $T = 20$ K. Similar values of $\gamma(T)$ also were obtained for other samples as a result of their consistent behavior in the upper critical field [see Fig.4(a)]. The anisotropy of the upper critical field near T_c can be associated with its electronic band structure. Observation of $\gamma \sim 8$ near T_c might suggest a quasi-two-dimensional electronic structure for $Tl_{0.58}Rb_{0.42}Fe_{1.72}Se_2$, which is compatible with the large resistive anisotropy in the normal state ($\rho_c/\rho_{ab} \sim 30$) (Ref. 11). An anisotropy of $\gamma \sim 8$ near T_c in $Tl_{0.58}Rb_{0.42}Fe_{1.72}Se_2$ is relatively large among the FeSCs,[20–25] but it is close to that of the 1111 compounds.[24] Nevertheless, in all these systems, the superconducting properties tend to be more isotropic at low temperatures, which would be compatible with the isotropiclike superconducting energy gaps observed around 15 K in the ARPES experiments.[16–19]

In order to further characterize the nature of the anisotropy in $Tl_{0.58}Rb_{0.42}Fe_{1.72}Se_2$, we have measured the angular dependence of the electrical resistivity $\rho(T)$ at various magnetic fields. Figure 5 plots the angular dependence of $T_c(\theta)$, where θ is the angle between the magnetic field and the c axis of the sample as marked in the figure.

According to the single-band anisotropic Ginzburg-Landau (G-L) theory,[35,36] the angular dependence of the upper critical field can be scaled by

$$\mu_0 H_{c2}^{\mathrm{GL}}(\theta) = \mu_0 H_{c2}/\sqrt{\cos^2(\theta) + \gamma^{-2}\sin^2(\theta)}, \quad (3)$$

where $\gamma = (m_{ab}/m_c)^{1/2} = H_{c2}^{\mathbf{H}\perp c}/H_{c2}^{\mathbf{H}\parallel c}$. Here, m_{ab} and m_c are the effective masses of electrons for the in-plane and out-of-plane motions, respectively. In the case where H_{c2} is a linear function of temperature, the angular dependence of $\mu_0 H_{c2}(\theta)$ can be converted to that of T_c by[37]

$$T_c(\theta) = T_{c0} + H/\left(\partial H_{c2}^{\mathbf{H}\parallel c}/\partial T\right)\sqrt{\cos^2(\theta) + \gamma^{-2}\sin^2(\theta)}, \quad (4)$$

where T_{c0} is the zero-field superconducting transition temperature and H is the applied magnetic field. In our case, the upper critical field near T_c indeed shows nearly linear temperature dependence for both $\mathbf{H} \perp c$ and $\mathbf{H} \parallel c$. Therefore, one can estimate the anisotropic parameter γ from the angular dependence of $T_c(\theta)$. It was shown that a single-band anisotropic model properly can describe the angular dependence of $\mu_0 H_{c2}$ in a multiband system at temperatures near T_c.[21,38] Indeed, $T_c(\theta)$ can be fitted nicely by Eq. (4) (see the solid lines in Fig. 5), indicating that, at least, in the low-field region, $T_c(\theta)$ can be described by the G-L theory and the anisotropic upper critical field is attributed to the effective-mass anisotropy in strongly coupled layered superconductors. Furthermore, the above fittings give $\gamma = 8.5$,7.3 and 6.3 for $\mu_0 H = 3$, 6 and 9 T, respectively. These values of $\gamma(\mu_0 H)$ are very close to those shown in the inset of Fig. 4 if we convert the magnetic fields to temperatures following the relation of $\mu_0 H_{c2}(T_c)$.

In comparison, the iron selenides show intrinsically similar properties of the upper critical field to the iron pnictide superconductors[20–25] but with a slightly enhanced anisotropy. These findings suggest that all these FeSCs might share the same characters of superconductivity. This is surprising because the electronic structure and the normal state of iron selenides seem to be very unique among the FeSCs. For example, both hole pockets and electron pockets are observed in iron pnictides,[19] but the hole pocket seems to be absent in iron selenides.[16–18] The nesting between the hole pockets and the electron pockets was regarded as a prerequisite factor for the forming of the $s^{\pm}$-pairing state,[39] a widely accepted proposal for the iron pnictide superconductors. Our findings of the universal behavior of $\mu_0 H_{c2}(T_c)$ in iron pnictides and selenides, therefore, urge us to check whether the missing hole pockets in iron selenides are intrinsic or are masked by other experimental factors, e.g., the phase separation or sample nonstoichiometry. If it is intrinsic, one probably needs to reconsider the order parameters and the pairing mechanism of the FeSCs in a unified picture.

IV. THERMALLY ACTIVATED FLUX FLOW

As already mentioned above, the superconducting transition of $Tl_{0.58}Rb_{0.42}Fe_{1.72}Se_2$ is broadened significantly upon applying a magnetic field (see Figs. 2 and 3). Similar features were observed previously in other layered superconductors, including the cuprates[40,41] and the 1111-type iron pnictides,[27–29] which were interpreted in terms of the energy dissipation caused by the vortices' motion. In general, both thermally activated flux flow (TAFF) and superconducting critical fluctuations may broaden the resistive superconducting transition in a magnetic field. The importance of thermal fluctuations is measured by the Ginzburg number $G_i = \frac{1}{2}(\gamma T_c / H_c^2 \xi_{ab}^3)^2$, where H_c is the thermal dynamic critical field and ξ_{ab} is the coherence length in the *ab* plane. In $Tl_{0.58}Rb_{0.42}Fe_{1.72}Se_2$, the relatively large anisotropic parameter γ near T_c and the short coherence length ($\xi \simeq 2.1$ nm) yield a large Ginzburg number G_i and a soft vortex matter. As a result, thermal fluctuations may become important enough to overcome the elastic energy of the vortex lattice in a large part of the magnetic-field-temperature-phase diagram, melting the vortex lattice into a liquid. On the other hand, the critical fluctuations may play a less dominant role here. Therefore, in the following, we try to interpret the resistive broadening in terms of the thermally activated flux flows, which actually give a rather good description for our experimental data. Further measurements are also under way in order to elucidate the possible effect of superconducting fluctuations.

According to the TAFF model,[42] the resistivity $\rho(T,H)$ can be expressed as

$$\rho(T,H) = (2\nu_0 LH/J)\sinh[JHVL/T]e^{-J_{c0}HVL/T}, \quad (5)$$

where ν_0 is the attempt frequency for the flux-bundle hopping, L is the hopping distance, J is the applied current density, J_{c0} is the critical current density in the absence of flux creep, and V is the bundle volume. In the limit of $JHVL/T \ll 1$, Eq. (5)

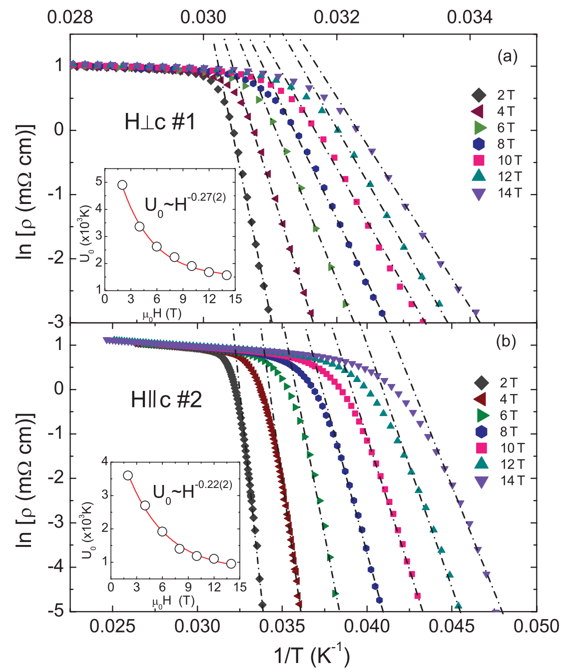

FIG. 6. (Color online) Arrhenius plot of $Tl_{0.58}Rb_{0.42}Fe_{1.72}Se_2$ at various magnetic fields: (a) $\mathbf{H} \perp c$; (b) $\mathbf{H} \parallel c$. The inset shows the thermally activated energy $U_0(H)$ obtained from the slope of the Arrhenius plot. The solid lines are fitted to $U_0(H) \approx H^{-n}$ with $n = 0.27 \pm 0.02$ and 0.22 ± 0.02 for $\mathbf{H} \perp c$ and $\mathbf{H} \parallel c$, respectively.

can be simplified as

$$\rho(T,H) = (2\rho_c U/T)e^{-U/T}, \quad (6)$$

where $U = J_{c0}HVL$ is the thermally activated energy and $\rho_c = \nu_0 LH/J_{c0}$. Assuming that $2\rho_c U/T$ is a temperature-independent constant, noted as ρ_{0f}, and $U = U_0(1 - T/T_c)$, then Eq. (6) can be simplified to the Arrhenius relation,

$$\ln \rho(T,H) = \ln \rho_{0f} - U_0(H)/T + U_0(H)/T_c. \quad (7)$$

Thus, the apparent activation energy $U_0(H)$ could be extracted from the slopes of the Arrhenius plots, i.e., the plot of $\ln \rho$ vs $1/T$.

In order to study such a possible vortex motion in $Tl_{0.58}Rb_{0.42}Fe_{1.72}Se_2$, we plot the electrical resistivity ρ as a function of $1/T$ on a semilogarithmic scale at various magnetic fields (see Fig. 6). It is clear that the Arrhenius relation holds over a wide temperature range for both $\mathbf{H} \perp c$ and $\mathbf{H} \parallel c$, suggesting that the TAFF model may nicely describe the field-induced resistive broadening in $Tl_{0.58}Rb_{0.42}Fe_{1.72}Se_2$. Following $U_0(H) = -d \ln \rho / d(1/T)$, the apparent activation energy $U_0(H)$ then can be determined from the slope of the linear parts in Fig. 6. For example, this yields $U_0 \approx 4900$ K for $\mathbf{H} \perp c$ and 3607 K for $\mathbf{H} \parallel c$ at 2 T. The derived values of $U_0(H)$ are plotted as a function of the field in the insets of Fig. 6: (a) $\mathbf{H} \perp c$ and (b) $\mathbf{H} \parallel c$, which follow a power law of $U_0(H) \sim H^{-n}$. The fittings give $n = 0.27 \pm 0.02$ for $\mathbf{H} \perp c$ and 0.22 ± 0.02 for $\mathbf{H} \parallel c$, indicating that the pinning force may have a weak-orientation dependence. The derived values of $U_0(H)$ are slightly larger than those of some 1111-type iron pnictides, e.g., $NdFeAsO_{0.7}F_{0.3}$ (Ref. 27) and $CeFeAsO_{0.9}F_{0.1}$ (Ref. 28) but are smaller than those of $SmFeAsO_{0.85}$ (Ref. 29) and $YBa_2Cu_3O_{7-\delta}$ (Ref. 41), indicating a moderate pinning force among the cuprates and the FeSCs. Note that, in the 122-type iron pnictides where $\gamma \simeq 2$ near T_c, the range of the vortex-liquid state is very narrow and no significant broadening of the resistive superconducting transition has been observed in a magnetic field.[20,43]

V. CONCLUSION

The upper critical field $\mu_0 H_{c2}(T_c)$, its anisotropy $\gamma(T)$, and the vortex motion of the newly discovered $Tl_{0.58}Rb_{0.42}Fe_{1.72}Se_2$ have been studied by measuring the field, temperature, and angular dependences of the electrical resistivity. We found that this compound shows a large upper critical field [$\mu_0 H_{c2}^{\mathbf{H}\parallel c}(0\ \mathrm{K}) \simeq 60$ T, $\mu_0 H_{c2}^{\mathbf{H}\perp c}(18\ \mathrm{K}) \simeq 60$ T] with a moderate anisotropy near T_c. The anisotropic parameter decreases with decreasing temperature, reaching $\gamma(20\ \mathrm{K}) \sim 2$. Analysis based on the WHH model indicates that the upper critical field is limited orbitally for $\mathbf{H} \parallel c$ but, likely, is limited by the spin-paramagnetic effect for $\mathbf{H} \perp c$. These properties remarkably resemble those of iron pnictide superconductors, suggesting that all the Fe-based superconductors may bear similar characteristics and, therefore, may provide restrictions on the theoretical model. Similar to the cuprates and the 1111 series of iron pnictides, thermally activated flux flow might be responsible for the tail structure of the resistive transition below T_c, and the derived thermal activation energies are compatible with those of the 1111-type iron pnictides.

ACKNOWLEDGMENTS

Work at ZJU was supported by the National Science Foundation of China (Grants No. 10874146 and No. 10934005), the National Basic Research Program of China (973 Program) (Grants No. 2009CB929104 and No. 2011CBA00103), the PCSIRT of the Ministry of Education of China, Zhejiang Provincial Natural Science Foundation of China, and the Fundamental Research Funds for the Central Universities. Work at LANL was performed under the auspices of the National Science Foundation, the Department of Energy, and the State of Florida. B.M. was supported by the US Department of Energy, Basic Energy Sciences, Materials Sciences and Engineering Division.

*hqyuan@zju.edu.cn

[1] For reviews, see, e.g., Z. A. Ren and Z. X. Zhao, Adv. Mater. **21**, 4584 (2009); D. C. Johnston, Adv. Phys. **59**, 803 (2010); J. Paglione and R. L. Greene, Nature Phys. **6**, 645 (2010); P. M. Aswathy, J. B. Anooja, P. M. Sarun, and U. Syamaprasad, Supercond. Sci. Technol. **23**, 073001 (2010).

[2] J. Dong, H. J. Zhang, G. Xu, Z. Li, G. Li, W. Z. Hu, D. Wu, G. F. Chen, X. Dai, J. L. Luo, Z. Fang, and N. L. Wang, Europhys. Lett. **83**, 27006 (2008); D. J. Singh and M. H. Du, Phys. Rev. Lett. **100**, 237003 (2008).

[3] Q. Si and E. Abrahams, Phys. Rev. Lett. **101**, 076401 (2008); K. Seo, B. A. Bernevig, and J. P. Hu, Phys. Rev. Lett. **101**, 206404 (2008); J. H. Dai, Q. M. Si, J. X. Zhu, and E. Abrahams, Proc. Natl. Acad. Sci. USA **106**, 4118 (2009).

[4] S. P. Kou, T. Li, and Z. Y. Weng, Europhys. Lett. **88**, 17010 (2009); M. D. Johannes and I. I. Mazin, Phys. Rev. B **79**, 220510(R) (2009); L. de'Medici, S. R. Hassan, M. Capone, and X. Dai, Phys. Rev. Lett. **102**, 126401 (2009).

[5] H. Q. Yuan, L. Jiao, F. F. Balakirev, J. Singleton, C. Setty, J. P. Hu, T. Shang, L. J. Li, G. H. Cao, Z. A. Xu, B. Shen, and H. H. Wen, e-print arXiv:1102.5476.

[6] S. J. Moon, J. H. Shin, D. Parker, W. S. Choi, I. I. Mazin, Y. S. Lee, J. Y. Kim, N. H. Sung, B. K. Cho, S. H. Khim, J. S. Kim, K. H. Kim, and T. W. Noh, Phys. Rev. B **81**, 205114 (2010).

[7] J. G. Guo, S. F. Jin, G. Wang, S. C. Wang, K. X. Zhu, T. T. Zhou, M. He, and X. L. Chen, Phys. Rev. B **82**, 180520 (2010).

[8] A. Krzton-Maziopa, Z. Shermadini, E. Pomjakushina, V. Pomjakushin, M. Bendele, A. Amato, R. Khasanov, H. Luetkens, and K. Conder, J. Phys.: Condens. Matter **23**, 052203 (2011).

[9] A. F. Wang, J. J. Ying, Y. J. Yan, R. H. Liu, X. G. Luo, Z. Y. Li, X. F. Wang, M. Zhang, G. J. Ye, P. Cheng, Z. J. Xiang, and X. H. Chen, Phys. Rev. B **83**, 060512 (2011).

[10] M. H. Fang, H. D. Wang, C. H. Dong, Z. J. Li, C. M. Feng, J. Chen, and H. Q. Yuan, Europhys. Lett. **94**, 27009 (2011).

[11] H. D. Wang, C. H. Dong, Z. J. Li, Q. H. Mao, S. S. Zhu, C. M. Feng, H. Q. Yuan, and M. H. Fang, Europhys. Lett. **93**, 47004 (2011).

[12] R. H. Liu, X. G. Luo, M. Zhang, A. F. Wang, J. J. Ying, X. F. Wang, Y. J. Yan, Z. J. Xiang, P. Cheng, G. J. Ye, Z. Y. Li, and X. H. Chen, Europhys. Lett. **94**, 27008 (2011).

[13] Z. Shermadini, A. Krzton-Maziopa, M. Bendele, R. Khasanov, H. Luetkens, K. Conder, E. Pomjakushina, S. Weyeneth, V. Pomjakushin, O. Bossen, and A. Amato, Phys. Rev. Lett. **106**, 117602 (2011).

[14] W. Bao, G. N. Li, Q. Huang, G. F. Chen, J. B. He, M. A. Green, Y. Qiu, D. M. Wang, and J. L. Luo, e-print arXiv:1102.3674; W. Bao, Q. Huang, G. F. Chen, M. A. Green, D. M. Wang, J. B. He, X. Q. Wang, and Y. Qiu, Chin. Phys. Lett. **28**, 086104 (2011).

[15] Y. J. Yan, M. Zhang, A. F. Wang, J. J. Ying, Z. Y. Li, W. Qin, X. G. Luo, J. Q. Li, J. P. Hu, and X. H. Chen, e-print arXiv:1104.4941.

[16] Y. Zhang, L. X. Yang, M. Xu, Z. R. Ye, F. Chen, C. He, H. C. Xu, J. Jiang, B. P. Xie, J. J. Ying, X. F. Wang, X. H. Chen, J. P. Hu, M. Matsunami, S. Kimura, and D. L. Feng, Nature Mater. **10**, 273 (2011).

[17] X. P. Wang, T. Qian, P. Richard, P. Zhang, J. Dong, H. D. Wang, C.-H. Dong, M. H. Fang, and H. Ding, Europhys. Lett. **93**, 57001 (2011).

[18] D. X. Mou, S. Y. Liu, X. W. Jia, J. F. He, Y. Y. Peng, L. Zhao, L. Yu, G. D. Liu, S. L. He, X. L. Dong, J. Zhang, H. D. Wang, C. H. Dong, M. H. Fang, X. Y. Wang, Q. J. Peng, Z. M. Wang, S. J. Zhang, F. Yang, Z. Y. Xu, C. T. Chen, and X. J. Zhou, Phys. Rev. Lett. **106**, 107001 (2011).

[19] H. Ding, P. Richard, K. Nakayama, K. Sugawara, T. Arakane, Y. Sekiba, A. Takayama, S. Souma, T. Sato, T. Takahashi, Z. Wang, X. Dai, Z. Fang, G. F. Chen, J. L. Luo, and N. L. Wang, Europhys. Lett. **83**, 47001 (2008); V. Brouet, M. Marsi, B. Mansart, A. Nicolaou, A. Taleb-Ibrahimi, P. Le Fèvre, F. Bertran, F. Rullier-Albenque, A. Forget, and D. Colson, Phys. Rev. B **80**, 165115 (2009).

[20]H. Q. Yuan, J. Singleton, F. F. Balakirev, S. A. Baily, G. F. Chen, J. L. Luo, and N. L. Wang, Nature (London) **457**, 565 (2009).
[21]S. A. Baily, Y. Kohama, H. Hiramatsu, B. Maiorov, F. F. Balakirev, M. Hirano, and H. Hosono, Phys. Rev. Lett. **102**, 117004 (2009).
[22]M. H. Fang, J. H. Yang, F. F. Balakirev, Y. Kohama, J. Singleton, B. Qian, Z. Q. Mao, H. D. Wang, and H. Q. Yuan, Phys. Rev. B **81**, 020509 (2010).
[23]N. Kurita, K. Kitagawa, K. Matsubayashi, A. Kismarahardja, E. S. Choi, J. S. Brooks, Y. Uwatoko, S. Uji, and T. Terashima, J. Phys. Soc. Jpn. **80**, 013706 (2011); K. Cho, H. Kim, M. A. Tanatar, Y. J. Song, Y. S. Kwon, W. A. Coniglio, C. C. Agosta, A. Gurevich, and R. Prozorov, Phys. Rev. B **83**, 060502 (2011); J. L. Zhang, L. Jiao, F. F. Balakirev, X. C. Wang, C. Q. Jin, and H. Q. Yuan, *ibid.* **83**, 174506 (2011).
[24]H. S. Lee, M. Bartkowiak, J. H. Park, J. Y. Lee, J. Y. Kim, N. H. Sung, B. K. Cho, C. U. Jung, J. S. Kim, and H. J. Lee, Phys. Rev. B **80**, 144512 (2009).
[25]V. A. Gasparov, L. Drigo, A. Audouard, D. L. Sun, C. T. Lin, S. L. Bud'ko, P. C. Canfield, F. Wolff-Fabris, and J. Wosnitza, JETP Lett. **93**, 667 (2011).
[26]J. Guo, L. L. Sun, C. Zhang, J. G. Guo, X. L. Chen, Q. Wu, D. C. Gu, P. W. Gao, X. Dai, and Z. X. Zhao, e-print arXiv:1101.0092.
[27]J. Jaroszynski, F. Hunte, L. Balicas, Y.-j. Jo, I. Raičevič, A. Gurevich, D. C. Larbalestier, F. F. Balakirev, L. Fang, P. Cheng, Y. Jia, and H. H. Wen, Phys. Rev. B **78**, 174523 (2008).
[28]M. Shahbazi, X. L. Wang, C. Shekhar, O. N. Srivastava, and S. X. Dou, Supercond. Sci. Technol. **23**, 10500 (2010).
[29]Y. Z. Zhang, Z. A. Ren, and Z. X. Zhao, Supercond. Sci. Technol. **22**, 065012 (2009); H.-S. Lee, M. Bartkowiak, J. S. Kim, and H.-J. Lee, Phys. Rev. B **82**, 104523 (2010).
[30]U. Welp, W. K. Kwok, G. W. Crabtree, K. G. Vandervoort, and J. Z. Liu, Phys. Rev. Lett. **62**, 1908 (1989); M. S. Osofsky, R. J. Soulen, Jr., S. A. Wolf, J. M. Broto, H. Rakoto, J. C. Ousset, G. Coffe, S. Askenazy, P. Pari, I. Bozovic, J. N. Eckstein, and G. F. Virshup, *ibid.* **71**, 2315 (1993).
[31]E. D. Mun, M. M. Altarawneh, C. H. Mielke, V. S. Zapf, R. Hu, S. L. Bud'ko, and P. C. Canfield, Phys. Rev. B **83**, 100514 (2011).
[32]H. C. Lei and C. Petrovic, Europhys. Lett. **95**, 57006 (2011).
[33]N. R. Werthamer, E. Helfand, and P. C. Hohenberg, Phys. Rev. **147**, 295 (1966).
[34]A. M. Clogston, Phys. Rev. Lett. **9**, 266 (1962); B. S. Chandrasekhar, Appl. Phys. Lett. **1**, 7 (1962).
[35]D. R. Tilley, Proc. Phys. Soc. London **86**, 289 (1965).
[36]G. Blatter, V. B. Geshkenbein, and A. I. Larkin, Phys. Rev. Lett. **68**, 875 (1992).
[37]U. Welp, W. K. Kwok, G. W. Crabtree, K. G. Vandervoort, and J. Z. Liu, Phys. Rev. B **40**, 5263 (1989).
[38]A. Gurevich, Phys. Rev. B **67**, 184515 (2003).
[39]I. I. Mazin and J. Schmalian, Phys. C **469**, 614 (2009).
[40]W. K. Kwok, S. Fleshler, U. Welp, V. M. Vinokur, J. Downey, G. W. Crabtree, and M. M. Miller, Phys. Rev. Lett. **69**, 3370 (1992).
[41]T. T. M. Palstra, B. Batlogg, R. B. van Dover, L. F. Schneemeyer, and J. V. Waszczak, Phys. Rev. B **41**, 6621 (1990).
[42]G. Blatter, M. V. Feigel'Man, V. B. Geshkenbein, A. I. Larkin, and V. M. Vinokur, Rev. Mod. Phys. **66**, 1125 (1994).
[43]B. Maiorov, T. Katase, S. A. Baily, H. Hiramatsu, T. G. Holesinger, H. Hosono, and L. Civale, Supercond. Sci. Technol. **24**, 055007 (2011).